



RESEARCH PAPER

# Modeling Drug Dissolution in 3-Dimensional Space

Chi So<sup>1</sup> · Po-Chang Chiang<sup>1</sup> · Chen Mao<sup>1</sup>

Received: 25 January 2022 / Accepted: 21 April 2022 / Published online: 26 April 2022

© The Author(s), under exclusive licence to Springer Science+Business Media, LLC, part of Springer Nature 2022

## Abstract

**Purpose** The purpose of the study is to present a mathematical model capable of describing drug particle dissolution in 3-dimensional (3D) space, and to provide experimental model verification. Through this study, we also aim to elaborate limitations of the classic, 1D-based Nernst-Brunner formalism in dissolution modeling.

**Methods** The 3D dissolution model was derived by treating the dissolution of a spherical particle as a diffusion-driven process, and by solving Fick's 2<sup>nd</sup> law of diffusion in spherical coordinates using numerical methods. The resulting model was experimentally verified through analyzing the dissolution behavior of single succinic acid particles in un-stirred water droplet under polarized light microscopy, in combination with image segmentation techniques.

**Results** A set of working equations was developed to describe drug particle dissolution in 3D space. The predicted dissolution time and profile are in good agreement with the experimental results. The model clearly shows that the concentration gradient within the diffusion layer, in realistic 3D condition, must not be a constant value as implicated in the Nernst-Brunner formalism. The actual concentration profile is a hyperbola, and the concentration gradient at the surface of the particle can be significantly higher than the classic 1D-based dissolution model.

**Conclusion** The study demonstrates that the classic, 1D-based dissolution models may lead to significant under-estimation of drug dissolution rates. In contrast, modeling dissolution in 3D space yields more reliable results. This study merits further development of comprehensive 3D drug dissolution models, by considering polydispersed particle ensemble and imposing the changes of diffusion layer thickness during dissolution.

**KEY WORDS** drug dissolution · diffusion · Fick's law of diffusion · mathematical modeling · Nernst-Brunner equation · Noyes-Whitney equation

## INTRODUCTION

Dissolution of drug particles is among the most crucial steps underlying the performance of solid dosage forms (1, 2). Modeling of drug particle dissolution dated back to the late nineteenth century, when Arthur Noyes and Willis Whitney published the esteemed article, demonstrating that the dissolution rate is linearly proportional to the difference between the drug solubility and the concentration of the bulk solution (3). This ground-breaking work further evolved into the well-known Nernst-Brunner equation,  $\frac{dM}{dt} = \frac{SD}{h}(C_s - C_t)$ , by treating dissolution as a diffusion-controlled process using Fick's first law of diffusion (4, 5). Here,  $\frac{dM}{dt}$  denotes the rate

of drug release,  $S$  is the surface area of the particles,  $D$  is the drug diffusion coefficient,  $h$  is the thickness of the diffusion layer, and  $(C_s - C_t)$  is the difference between the drug solubility and the bulk fluid concentration at time  $t$ . Although several alternative mechanisms of dissolution were later proposed (6, 7), the Nernst-Brunner formalism remains to be the dominant model describing the drug particle dissolution behavior in the pharmaceutical industry to date (8, 9).

A key assumption underlying the Nernst-Brunner formalism is the presence of the static diffusion layer immediately adjacent to the surface of the particles, in which the diffusion of the drug prevails. While the thickness ( $h$ ) of the layer cannot be measured in reality, it is a manifestation of the resistance to mass transfer of drug molecules in dissolution. Based on fluid dynamics models, for a system where convective mass transfer takes place (such as drug particles suspended in fluid), the diffusion layer thickness

✉ Chen Mao  
mao.chen@gene.com

<sup>1</sup> Small Molecule Pharmaceutical Sciences, Genentech, Inc.,  
1 DNA Way, South San Francisco, CA 94080, USA

is calculated as the ratio of the characteristic length ( $L$ ) to the Sherwood number ( $Sh$ ) (10). For spherical particles,  $L$  is considered to be equal to the diameter of the particle, and the  $Sh$  can be determined by the Ranz-Marshall equation ( $Sh = 2 + 0.6 * Re^{1/2} * Sc^{1/3}$ ), where  $Re$  is the Reynolds number and  $Sc$  is the Schmidt number (11). When there is no convective mass transfer,  $Sh$  becomes 2 because  $Re$  is zero due to the absence of fluid flow, and  $h$  is therefore equal to the radius of the particle.

Although  $h$  is computed by considering the mass transfer in 3-dimensional (3D) space, as described by the Ranz-Marshall Eq. (11), the Nernst-Brunner equation itself was derived with an underlying assumption that the diffusion takes place under the 1-dimensional (1D) condition (12). This is because only under 1D, can the drug concentration gradient across the diffusion layer be a constant value and denoted as  $(C_s - C_i)/h$ . However, realistic drug particle dissolution is not a 1D phenomenon, as actual drug dissolution occurs in a 3D space. This limitation was raised by Wang and Flanagan (13, 14), who critically pointed out that the drug concentration gradient of a spherical particle within the diffusion layer must not be a constant value, considering the 3D condition. By solving Fick's first law using a non-constant, distance-dependent concentration gradient, Wang and Flanagan showed that the widely used "cubic root law" in drug dissolution modeling, which was derived with from the Nernst-Brunner formalism (15, 16), is valid only when the particle size is substantially greater than the diffusion layer thickness (13). In other words, modeling of drug particle dissolution using the classic, 1D approach, though widely adopted, may misrepresent the dissolution behavior in reality.

In light of this constraint, we here present a model capable of describing drug particle dissolution under 3D condition, but still following the same fundamental principle underpinning the Nernst-Brunner formalism (namely, dissolution is driven by diffusion within the diffusion layer). Specifically, we propose that the drug particle dissolution behavior can be modeled by solving Fick's second law of diffusion in 3D space. Solving Fick's second law gives rise to the drug concentration as the function of time and location within the diffusion layer. Once a solution is identified, the drug dissolution rate can be subsequently obtained by subjecting the drug concentration to Fick's first law of diffusion. This approach has an advantage over Wang and Flanagan's method (13), by which only the Fick's first law was employed. The advantage arises from the fact that Fick's first law is constrained to describing the steady state diffusion only, whereas Fick's second law covers both the steady and non-steady state processes. Hence, a model derived from Fick's second law may provide a more holistic description of the drug particle dissolution

process, and potentially shed light on how drug properties and environmental conditions, such as particle size, solubility, or hydrodynamics, affect drug dissolution under the 3D consideration.

## Theoretical Section

### Deriving the General Particle Dissolution Model in 3D Based on Fick's Law of Diffusion

Similar to the principles underlying the Noyes-Whitney and Nernst-Brunner Eqs. (3–5), the particle dissolution model in 3D concerns the presence of a diffusion layer adjacent to the surface of the particle, in which the drug molecule is governed by Fick's law of diffusion, with the exception that the Fick's law is expressed in a 3D space. Considering a compound with the diffusion coefficient  $D$  in water, present as a spherical particle with the radius of  $a$ . It is appropriate to study the dissolution in spherical coordinates for simplicity of derivation. To this end, Fick's second law of diffusion in the 3D spherical coordinates is employed. The law is expressed as (17):

$$\frac{\partial C}{\partial t} = \frac{D}{r^2} \left[ \frac{\partial}{\partial r} \left( r^2 \frac{\partial C}{\partial r} \right) + \frac{1}{\sin \theta} \frac{\partial}{\partial \theta} \left( \sin \theta \frac{\partial C}{\partial \theta} \right) + \frac{1}{\sin^2 \theta} \frac{\partial^2 C}{\partial \phi^2} \right] \quad (1)$$

where  $\frac{\partial C}{\partial t}$  is the rate of drug concentration change anywhere in the diffusion layer during dissolution,  $t$  is time, and  $r$  is the radial distance from the origin,  $\theta$  is the polar angle, and  $\phi$  is the azimuthal angle. Assuming the diffusion is isotropic, Eq. 1 can be simplified due to spherical symmetry as:

$$\frac{\partial C}{\partial t} = D \frac{1}{r^2} \frac{\partial}{\partial r} \left( r^2 \frac{\partial C}{\partial r} \right) \quad (2)$$

The goal is therefore to find a solution for Eq. 2 considering the drug concentration  $C$  in the diffusion layer. Because Eq. 2 implies that  $C$  is a sole function of location  $r$  and time  $t$ , one can express  $C$  as a product form using the method of separation of variables:

$$C = C(r, t) = R(r)T(t) \quad (3)$$

Combining Eqs. 2 and 3 leads to:

$$R \frac{\partial T}{\partial t} = DT \frac{1}{r^2} \frac{\partial}{\partial r} \left( r^2 \frac{\partial R}{\partial r} \right) \quad (4)$$

Equation 4 can therefore be rearranged to allow  $R$  and  $T$  solved separately:

$$\frac{1}{R} \frac{1}{r^2} \frac{\partial}{\partial r} \left( r^2 \frac{\partial R}{\partial r} \right) = \frac{1}{DT} \frac{\partial T}{\partial t} \quad (5)$$

Introducing to Eq. 5 an arbitrary separation constant  $-k^2$ :

$$\frac{1}{R} \frac{1}{r^2} \frac{\partial}{\partial r} \left( r^2 \frac{\partial R}{\partial r} \right) = \frac{1}{DT} \frac{\partial T}{\partial t} = -k^2 \tag{6}$$

To solve for  $R$ , one is to apply the chain rule to the left-hand side of Equation 6:

$$\frac{1}{R} \left( \frac{\partial^2 R}{\partial r^2} + \frac{2}{r} \frac{\partial R}{\partial r} \right) = -k^2 \tag{7}$$

Equation 7 can be re-written in the form of Bessel’s differential equation in spherical coordinates (18):

$$r^2 \frac{\partial^2 R}{\partial r^2} + 2r \frac{\partial R}{\partial r} + [(kr)^2 - l(l + 1)]R = 0, \text{ of which } l = 0 \tag{8}$$

The solution of Eq. 8 is the zeroth order spherical Bessel function of the first kind:

$$R = j_0 = \frac{\sin(kr)}{kr} \tag{9}$$

Here, we demand that the values of  $R$  at the surface of the particle,  $R(a)$ , and at the edge of the diffusion layer,  $R(a + h)$ , are zero, so that the function  $R$  does not interfere with the boundary condition of the drug concentration  $C(r, t)$ . To meet this requirement, we found that  $k = \frac{n\pi}{h}, n = 1, 2, \dots$ . Therefore,  $R$  can be expressed as:

$$R(r) = \frac{\sin \left[ \frac{n\pi}{h} (r - a) \right]}{\frac{n\pi}{h} r} \tag{10}$$

where  $h$  is the diffusion layer thickness.

The function  $T(t)$  from Eq. 6 can also be solved as:

$$T(t) = e^{-Dk^2t} \tag{11}$$

Combining both solutions (Eqs. 3, 10, and 11) and applying the method of eigenfunction expansion lead to the final solution of the drug concentration  $C$ :

$$C(r, t) = R(r)T(t) = f(r) + \sum_n \frac{\sin \left[ \frac{n\pi}{h} (r - a) \right]}{r} b_n e^{-D \left( \frac{n\pi}{h} \right)^2 t} \tag{12}$$

where  $f(r)$  is the drug concentration at the steady state, and  $b_n$  are the Fourier series coefficients.

### Determining the Drug Concentration at the Steady State and Fourier Series Coefficients

In order to determine the steady state concentration  $f(r)$  and the Fourier series coefficients  $b_n$ , initial and

boundary conditions need to be imposed. Specifically, the following conditions with respect to the drug dissolution are given:

- 1) Sink condition is assumed. Namely, the drug concentration in the bulk (outside and interfacing the diffusion layer) remains zero.

$$C(a + h, t) = 0, t \geq 0$$

- 2) At time zero, the drug concentration in the diffusion layer is zero.

$$C(r, 0) = 0, r > a$$

- 3) The drug concentration at the surface of the particle is equal to the drug solubility ( $C_s$ ).  $C(a, t) = C_s, t \geq 0$

- 4) The drug concentration in the diffusion layer will reach a steady state.

$$C(r, t \rightarrow \infty) = f(r), a < r < a + h$$

At the steady state,  $\frac{\partial C}{\partial t} = D \frac{1}{r^2} \frac{\partial}{\partial r} \left( r^2 \frac{\partial C}{\partial r} \right) = 0$ . Therefore, it can be shown that steady state concentration  $f(r)$  takes the following form (17):

$$f(r) = \frac{A}{r} + B \tag{13}$$

where  $A$  and  $B$  are constants and can be obtained from the above boundary conditions:

$$A = \frac{C_s a(a + h)}{h}, \text{ and } B = -\frac{aC_s}{h} \tag{14}$$

The Fourier series coefficients  $b_n$  may be obtained by making use of the initial condition:  $C(r, 0) = 0, r > a$ . Applying the condition to Eq. 12–13 leads to:

$$C(r, 0) = \frac{A}{r} + B + \sum b_n \frac{\sin \left[ \frac{n\pi}{h} (r - a) \right]}{r} = 0 \tag{15}$$

Rearrange:

$$\sum b_n \left[ \frac{n\pi}{h} (r - a) \right] = \left( -\frac{A}{r} - B \right) \sin \left[ \frac{n\pi}{h} (r - a) \right] r \tag{16}$$

$b_n$  may therefore be solved using the orthogonality of the sine function (19) ( $\int_0^\pi \sin(mx) \sin(nx) dx = 0, n \neq m$ , and  $\int_0^\pi \sin(mx) \sin(nx) dx = \frac{\pi}{2}, n = m$ ). Equation 16 can thus be re-written by integrating across the diffusion layer as:

$$b_n \int_a^{a+h} \left[ \frac{n\pi}{h} (r - a) \right] dr = \int_a^{a+h} \left( -\frac{A}{r} - B \right) \sin \left[ \frac{n\pi}{h} (r - a) \right] r dr \tag{17}$$

Applying the orthogonality rule to Eq. 17 gives rise to  $b_n$ :

$$b_n = \frac{2}{n\pi} A(\cos n\pi - 1) + B[(a+h)\cos n\pi - a] \quad (18)$$

### Working Equations for Particle Dissolution in 3D

To summarize the preceding derivation, below is the set of working equations used to predict the drug dissolution in 3D space, derived completely from Fick's second law of diffusion in spherical coordinates. Specifically, the drug concentration  $C(r, t)$ , over the course of the dissolution under the sink condition, is expressed as:

$$C(r, t) = \frac{A}{r} + B + \sum_n b_n \frac{\sin\left[\frac{n\pi}{h}(r-a)\right]}{r} e^{-D\left(\frac{n\pi}{h}\right)^2 t} \quad (19)$$

where

$$A = \frac{C_s a(a+h)}{h}, \text{ and } B = -\frac{aC_s}{h} \quad (14)$$

and

$$b_n = \frac{2}{n\pi} A(\cos n\pi - 1) + B[(a+h)\cos n\pi - a] \quad (18)$$

The calculation is more precise when a large number of terms of the Fourier series are summed (i.e. a greater  $n$  value). In our calculation, we chose  $n = 4000$  to ensure sufficient Fourier series are summed, giving rise to reliable prediction results.

The dissolution rate  $\left(\frac{dM}{dt}\right)$  can be determined by employing Fick's first law:

$$J = -D \frac{\partial C}{\partial r} \Big|_{r=a} \quad (20)$$

where  $J$  is the flux at the surface of the particle ( $J = \frac{dM}{4\pi a^2 dt}$ ). Taking the derivative of Eq. 19 with respect to  $r$  leads to:

$$\frac{\partial C}{\partial r} \Big|_{r=a} = -\frac{A(t)}{a(t)^2} + \sum b_n \left(\frac{n\pi}{a(t)h}\right) e^{-D\left(\frac{n\pi}{h}\right)^2 t} \quad (21)$$

The drug dissolution rate can then be obtained by combining Eq. 20 and 21:

$$\frac{dM}{dt} = 4\pi D \left[ A(t) - \sum b_n \left(\frac{n\pi}{h} a(t)\right) e^{-D\left(\frac{n\pi}{h}\right)^2 t} \right] \quad (22)$$

Equation 22 was solved using variable order methods *ode15s* in MATLAB (20), with a quasi-constant step size implementation to handle the stiffness and to estimate the optimal initial step size. The relative and absolute residual tolerance are set to  $1 \times 10^{-10}$  to ensure model robustness under various conditions. This leads to the determination of the drug dissolution rate with known initial particle size, diffusion coefficient, and diffusion layer thickness.

Note that the coefficients  $A(t)$  and the particle radius  $a(t)$  are both considered as time-dependent functions in the equation.

In fact, the above derivation can be recognized as the preliminarily solution of a spherical one-phase Stefan problem, and it is possible that more accurate results may be obtained by employing large Stefan number and small time perturbation, as proposed in the literature (21, 22). However, for all practical purposes, the aforementioned solution is deemed sufficiently accurate to calculate drug particle dissolution in 3D.

## Materials and Methods

### Materials

Crystalline succinic acid ( $\geq 99\%$  fine grade, Sigma Aldrich) was used for the experimental model validation. The material was sieved prior to use, and only the fractions with the particle size between 300–500  $\mu\text{m}$  were selected for the dissolution study using optical microscopy. Particles of this size range is large enough to allow ample dissolution time for reliable data measurement, while still small enough to be fully captured by the instrument's field of view.

### Dissolution Visualization Using Polarized Light Microscopy

The dissolution of individual succinic acid particles in water was observed and recorded using a polarized light microscope (Olympus BX51, Olympus Corporation, Japan) coupled with a high-definition camera (DS-Fi3, Nikon Instruments, Japan). Specifically, a single succinic acid particle (particle size of 300–500  $\mu\text{m}$ ) was placed at the center of a glass slide without a coverslip. The glass slide was transferred to the microscope stage and the photomicrographs of the particle were collected under the time-lapse mode at 5-s or 10-s interval. A 10 $\times$  objective lens and a 10 $\times$  camera lens were employed, giving a visual magnification of 100 $\times$ . At the beginning of each experiment, 10  $\mu\text{L}$  of water was slowly and carefully pipetted onto the glass slide with the pipette tip positioned right above the particle. This exercise gave rise to a particle fully immersed in a water droplet spanning approximately 6 mm in diameter. It was critical that the water pipetting operation was performed with extraordinary care, so that the drug particle remained stationary inside the water droplet. The evolution of the particle size and shape in the water droplet was observed and recorded under the microscope until the particle fully dissolved. During the data collection, the illumination was reduced by dimming the light source and narrowing the aperture of the field iris diaphragm to minimize temperature elevation and water evaporation.

Consequently, the exposure time was increased to 220 ms to compensate the loss of illumination. The time-lapse data was first saved as source video files and then each frame was converted to a full-size image, using the Nikon® NIS-Elements image-processing platform.

### Image Analysis

To measure the particle dissolution rate, it is advisable to perform image segmentation so that the particle in each frame can be digitally extracted from the background for size measurement. As shown in Fig. 1A, the particle exhibits bright yellow-green color with a dark boundary, against the pink background (due to the presence of a full-wave plate in the light path). The segmentation was thus carried out by means of image thresholding within the HSV (Hue, Saturation, Value) color space, using the MATLAB® imaging processing toolbox. Specifically, the field of view (FOV) encompassing the particle from several representative images were chosen as the training set. The selected HSV color ranges were then applied to all frames for image thresholding (Fig. 1B), followed by the creation of the binary mask indicative of the whole particle extracted from the background (Fig. 1C). This technique gives rise to extracted particles largely representative of the original images. For certain images, bubbles or high surface asperity may cast shadows on the particle surface and hence lead to small extraction errors using the HSV image thresholding method (see Fig. 1A and 1C). Hence, additional image refinement techniques were implemented to yield more

faithful segmentation (Fig. 1D). These techniques include removing small object morphologically (*bwareopen*) and recovering the information loss from possible over-segmentation by filling small empty regions/holes (*imfill*). Following the image segmentation, the particle size in each frame was determined by calculating the area of the refined binary mask and converting it to the equivalent circular diameter (ECD).

### True Density Measurement

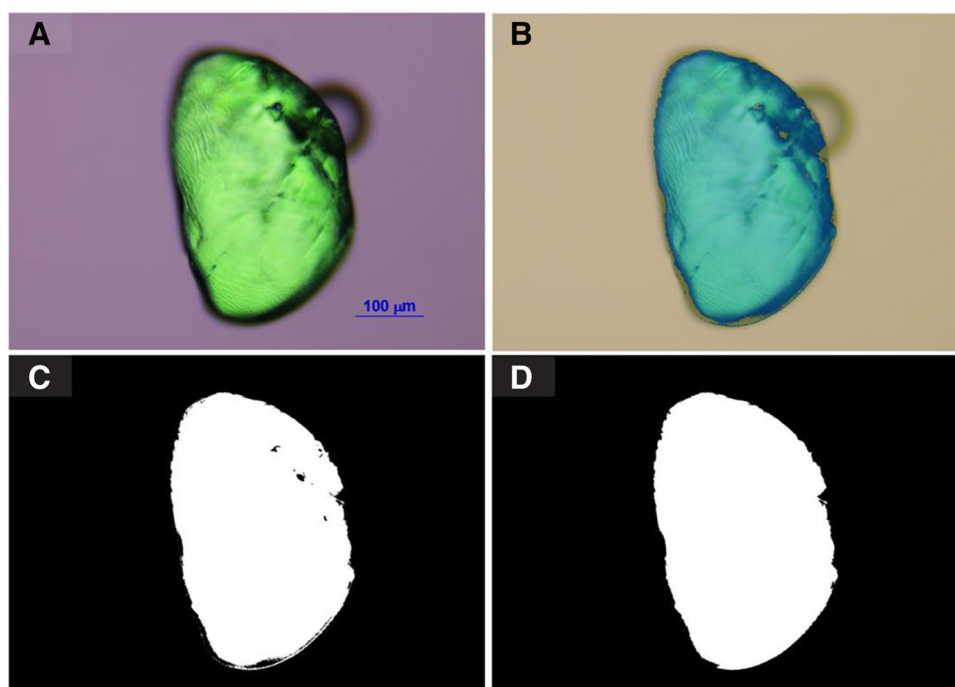
The true density of succinic acid particles was determined by helium-air pycnometry (AccuPyc II 1340, Micromeritics, Norcross, GA). Approximately 1.5 g of powder sample were loaded in the 3.5 cm sample container. The sample was left in the instrument for 10 min to reach the ambient temperature before the measurement started. Five air purge cycles and five sample measurement cycles were employed at the equilibration rate of 0.0050 psig/min. The density result was determined from an average value of all sample measurements.

### Results and Discussion

#### Nernst-Brunner Formalism Assumes Diffusion in 1D and May Under-Estimate Dissolution Rate

The Noyes-Whitney and Nernst-Brunner formalism is the commonly accepted model underlying drug dissolution for

**Fig. 1** Succinic acid particle observed under a polarized light microscope. Panel A: original photomicrograph; Panel B: after image thresholding; Panel C: binary mask; Panel D: refined binary mask.



decades. The model dictates that the drug dissolution rate,  $dM/dt$ , is linearly proportional to the particle surface area  $S$ , diffusion coefficient  $D$ , and a constant concentration gradient across the diffusion layer,  $(C_s - C_t)/h$  (or  $C_s/h$  under the sink condition). Here, the constant concentration gradient is a required condition stemming from the 1D assumption. To elaborate, Fick's second law of diffusion in 1D is expressed as  $\frac{\partial C}{\partial t} = D \frac{\partial^2 C}{\partial x^2}$ . Because  $\frac{\partial C}{\partial t} = 0$  at the steady state, the concentration gradient ( $\partial C/\partial x$ ) must be a constant value to satisfy Fick's second law. Namely, the concentration vs. distance profile across the diffusion layer is a straight line (Fig. 2).

Despite the simplicity of the 1D model, drug dissolution in reality occurs in the 3D space, and the diffusion of the drug molecules is not constrained to 1D. Considering an instance in which molecules diffuse radially into 3D space from the origin in spherical coordinates, shown in Fig. 3. As molecules move outward by an increment  $dr$ , the volume of the new space available for drug diffusion is  $\frac{4}{3}\pi(r + dr)^3 - \frac{4}{3}\pi r^3$ . In other words, the radial increment of the space available for diffusion is distance-dependent, and hence the concentration gradient in 3D space across the diffusion layer cannot be a constant value. Similar to the 1D condition, the steady state concentration gradient in 3D can also be determined, as  $\frac{\partial C}{\partial t} = D \frac{1}{r^2} \frac{\partial}{\partial r} \left( r^2 \frac{\partial C}{\partial r} \right) = 0$  considering the diffusion at the steady state in spherical coordinates. It can therefore be shown that the drug concentration is hyperbolically related to the distance within the diffusion layer ( $C = \frac{A}{r} + B$ , see Eq. 13) (Fig. 2). Under the sink condition, the steady state drug concentration gradient at surface of the particle is:  $\left. \frac{\partial C}{\partial r} \right|_{r=a} = \frac{C_s}{h} + \frac{C_s}{a}$ , which exceeds the concentra-

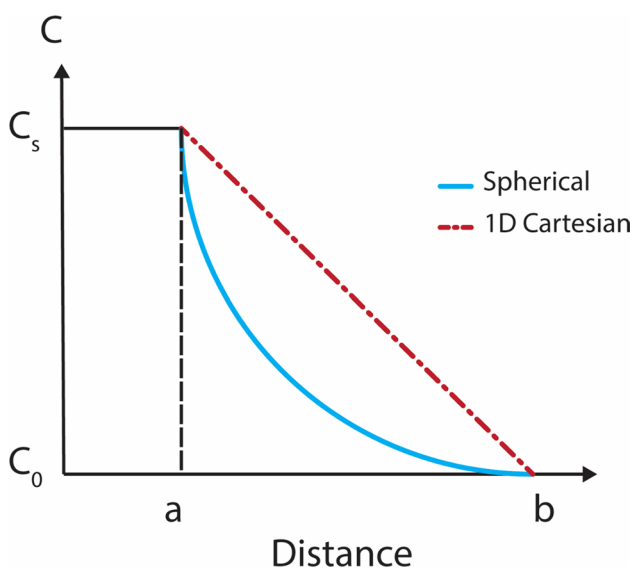


**Fig. 2** Schematic steady state concentration profiles within the diffusion layer (space between **a** and **b**) under the sink condition, obtained under the 1D (solid line) and 3D (dash line) considerations.

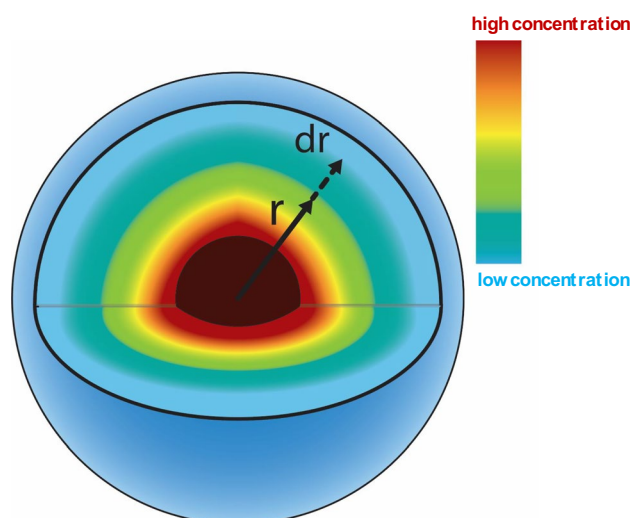


**Fig. 3** A diagram illustrating the dissolution of a drug particle in 3D space.

tion gradient under the 1D condition by an amount equal to  $C_s/a$ . In other words, this analysis shows that calculation using the Nernst-Brunner formalism, which assumes a constant concentration gradient, would lead to an under-estimation in drug dissolution rate, especially for drugs possessing large diffusion layer thickness or small particle size.

### Drug Dissolution Experiments Using Optical Microscopy

As previously noted, drug dissolution rate under the 3D condition can be calculated from a set of working equations provided in the [Theoretical Section](#), using adaptive numerical methods. Although the mathematical treatment is more intricate, modeling drug dissolution in 3D requires the same set of drug properties employed in the Nernst-Brunner equation. Namely, particle size (or surface area), equilibrium solubility, diffusion coefficient, and diffusion layer thickness. No additional drug properties are needed to enable the calculation.

To demonstrate the validity of the 3D drug dissolution model, experimental dissolution studies, using succinic acid particles, were carried out. While the particle size, room temperature solubility ( $C_s = 56$  mg/mL), and room temperature diffusion coefficient ( $D = 8.8 \times 10^{-10}$  m<sup>2</sup>/sec) of succinic acid can be accurately determined (23, 24), the diffusion layer thickness is largely particle size and hydrodynamics dependent and a degree of uncertainty is associated with its estimation (25). To overcome this limitation, a novel dissolution experiment setup was adopted. Specifically, an individual succinic acid particle was immersed in a water droplet on a glass slide, and the entire system was left intact while the dissolution process was observed under the microscope. The particle and the droplet remained fully stationary (un-stirred) during the course of the experiment. Under this

condition, water is not agitated and therefore the Reynolds number ( $Re$ ) is zero. This leads to the Sherwood number ( $Sh$ ) for spherical particles being equal to 2 based on the Ranz-Marshall Eq. (11). According to the fluid dynamic model, the diffusion layer thickness ( $h$ ) of the spherical particle is equal to the ratio of the particle diameter (i.e. characteristic length of spheres) to  $Sh$  (10). Consequently, for a static particle immersed in an un-stirred water droplet, as is the case in our experiments, the diffusion layer thickness is equivalent to the radius of the particle (a.k.a.  $h = a$ ). For this reason, we purposely produced a completely static dissolution system, thereby eliminating potential errors introduced from diffusion layer thickness estimation in an agitated system, in which the relative velocity of the fluid and particle flow has to be accounted for. A detailed account of the experimental setup can be found in the [Materials and Methods](#) Section.

### Drug Dissolution Rate can be Predicted Using the 3D Model

The progression of the succinic acid particle dissolution under the microscope is exemplified in Fig. 4. Succinic acid

was chosen for the study because the material possesses desirable aqueous solubility (56 mg/mL) and ideal particle size (300–500  $\mu\text{m}$ ), allowing reliable visualization and size measurement under optical microscopy and ample measurement time. Additionally, succinic acid particles exhibit aspect ratios close to unity, thus resembling “spherical” morphology assumed in our dissolution model. More than two dozen drug dissolution experiments were performed on individual succinic acid particles, and the collective results indicate that a majority of the particles fully dissolves within 5–10 min. Additionally, as Fig. 4 demonstrates, the dissolution of the succinic acid particle is generally isotropic, thus making it an ideal system for the dissolution model verification.

The evolution of the drug particle size during dissolution, derived from the segmented images described in the [Materials and Methods](#) Section, is exemplified in Fig. 5A. There is a good agreement between the experimental data and the predicted results, which was calculated by following the 3D dissolution model delineated in the [Theoretical Section](#). Both the simulated and experimental data show that the rate of the particle size decrease is not linear, and there is a clear

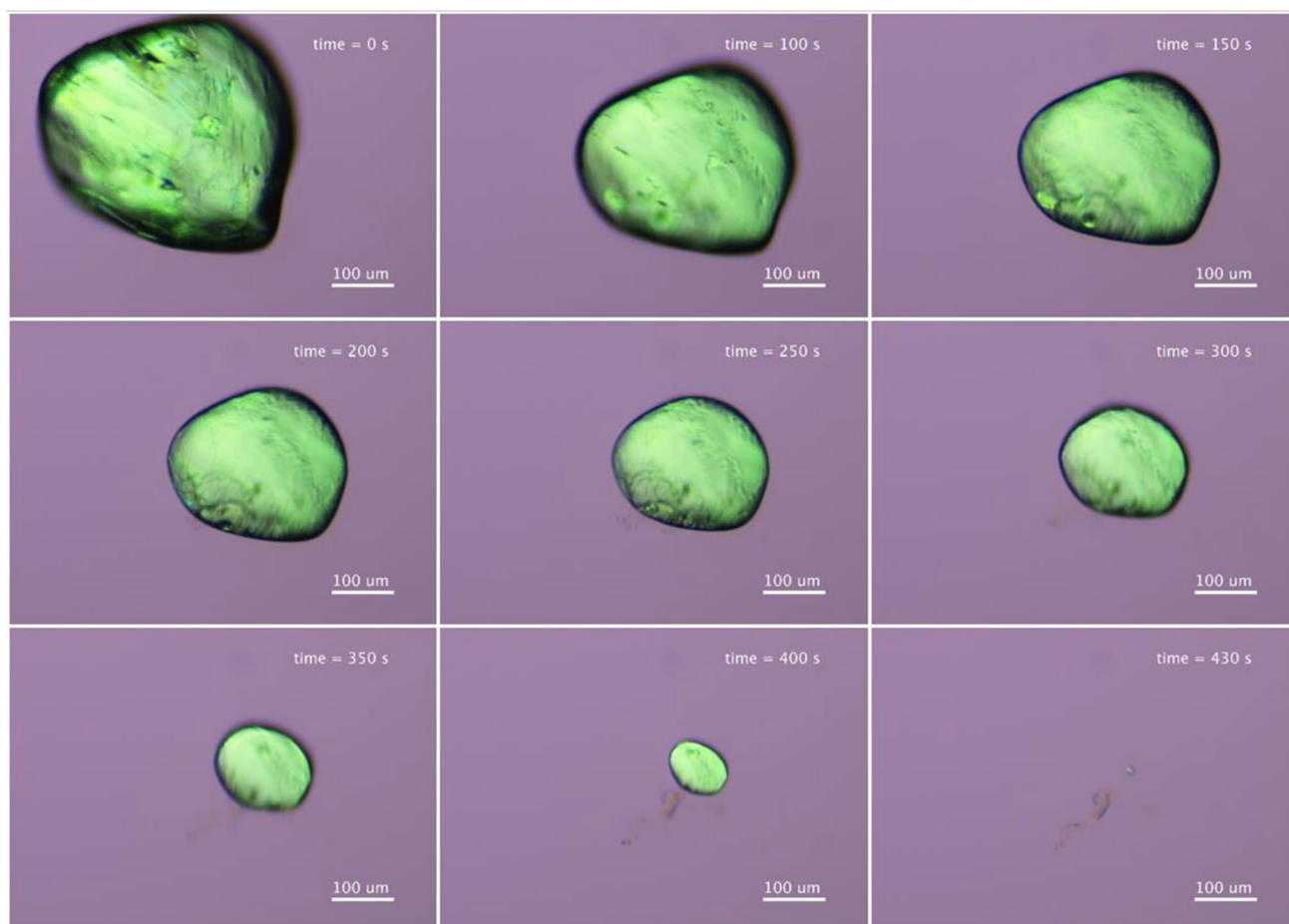
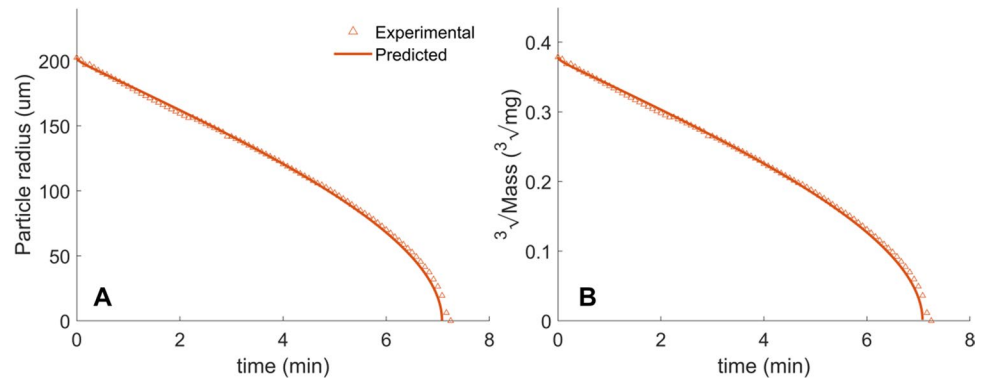


**Fig. 4** Photomicrographs capturing the evolution of a succinic particle size during the entire dissolution experiment.

**Fig. 5** Panel **A**: represented experimental and predicted (using the 3D model) particle size evolution for succinic acid particle dissolution; Panel **B**: plot of  $(\text{particle weight})^{1/3}$  vs. time for the same particle dissolution shown in Panel **A**.



acceleration of particle size reduction as the dissolution progresses (Fig. 5A). These phenomena conform to the previous analysis, because the steady state concentration gradient at the surface of the particle is inversely related to drug particle size ( $\left. \frac{\partial C}{\partial r} \right|_{r=a} = \frac{C_s}{h} + \frac{C_s}{a}$ ) under the sink condition. The concentration gradient therefore continues to increase with decreasing particle size, leading to an acceleration of drug dissolution especially toward the end, when the concentration gradient rises sharply.

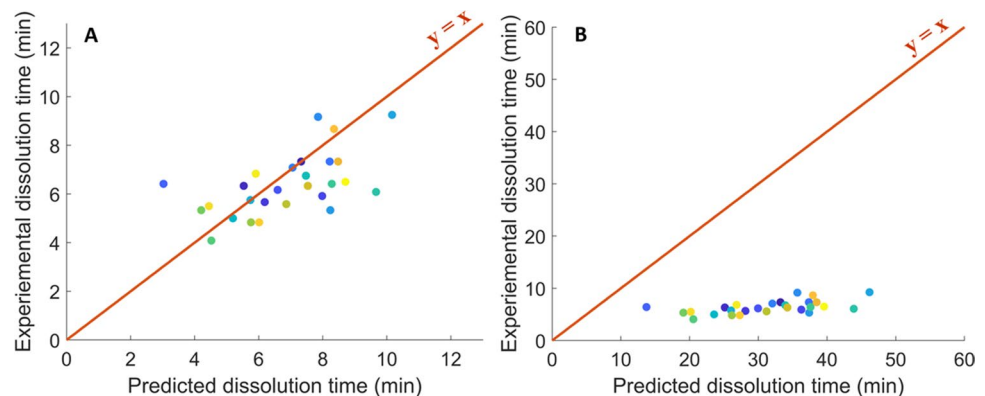
Additionally, because the weight of succinic acid particle  $W$  is proportional to its radius cubed ( $r^3$ ), the y-axis of Fig. 5A can be replaced with  $W^{1/3}$  (Fig. 5B). Simply put, the  $W^{1/3}$  vs. time curve is not a straight line. The significant departure from the linearity in Fig. 5B suggests that the succinic acid dissolution does not follow the widely-known “cube-root law” (15), which was derived on the basis of the 1D, Nernst-Brunner scheme. The deviation from the cube-root law in this experiment is well anticipated considering the drug dissolution in 3D. As Wang and Flanagan pointed out, the cube-root law is valid only when the particle size ( $a$ ) is much larger than the diffusion layer thickness ( $h$ ) (13). This is because under such circumstances ( $a \gg h$ ), the concentration gradient at the surface of the particle can be approximated as  $\left. \frac{\partial C}{\partial r} \right|_{r=a} = \frac{C_s}{h}$ . In other words, the 1D, Nernst-Brunner formalism re-assumes and the cube-root law

prevails. For our static dissolution system in which  $a = h$  at time zero, such condition cannot be met. Therefore the dissolution process is not expected to follow the cube-root law. Taken together, our observation further corroborates the drawback of drug dissolution modeling under the 1D consideration.

Collectively, there is a strong agreement between the predicted and experimental dissolution time, as shown in Fig. 6A, though slight scattering of data points was observed. This variation likely results from several factors: 1) because spherical particles are assumed in the model, any deviation from the perfect sphericity in actual succinic acid particles can lead to errors in surface area and therefore departure from the experimental dissolution time; and 2) illumination from the light source can cause slight temperature elevation of the water droplet, thereby increasing the diffusion coefficient and reducing dissolution time. Nevertheless, despite these experimental factors, the close proximity between the theoretical and experimental results, concerning both the dissolution time (Fig. 6A) and kinetics of dissolution profiles (Fig. 5A), suggests that modeling of dissolution in 3D can rationally reflect the actual dissolution behavior of particles.

For comparison, the succinic acid particle size evolution was also calculated concerning the 1D condition by employing the Nernst-Brunner formalism, using the same set of material properties. In sharp contrast to Fig. 6A, the

**Fig. 6** Correlation between the experimental and predicted dissolution time for all succinic acid particles tested. Panel **A**: predicted using the 3D model; Panel **B**: predicted using the Nernst-Brunner formalism.



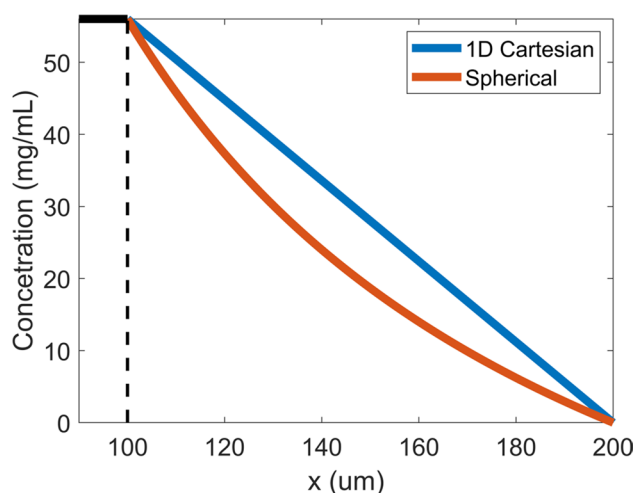


**Fig. 7** Calculated concentration profile of a succinic acid particle ( $d=200\ \mu\text{m}$ ) within the diffusion layer ( $h=100\ \mu\text{m}$ ), as described in the experiment.

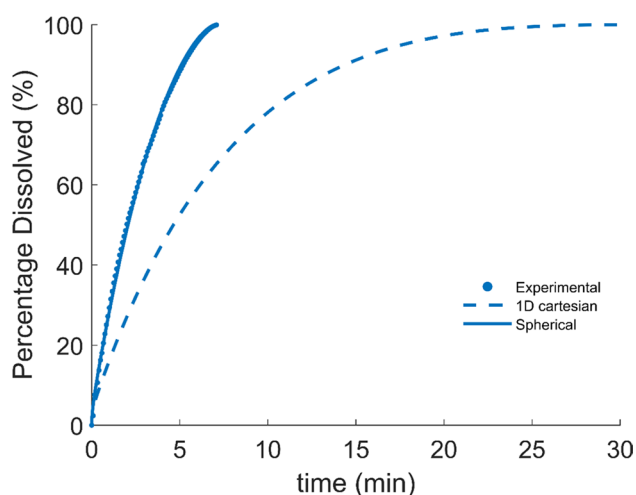


**Fig. 8** Representative dissolution profile of succinic acid particle (dots: experimental data; solid line: predicted profile from the 3D model; dash line: predicted profile from the Nernst-Brunner formalism).

predicted dissolution time obtained from the Nernst-Brunner formalism is substantially longer than experimental data (Fig. 6B). As previously discussed, the significant discrepancy between the predicted and experimental data primarily stems from the assumed presence of the linear concentration profile across the diffusion layer at the steady state (Fig. 7), which is a required outcome considering Fick's second law under the 1D condition. The actual concentration profile of succinic acid particle, considering the 3D space, is present in the form of hyperbola (Fig. 7), which is more precipitous than the linear concentration gradient profile obtained under the 1D scenario at the surface of the particles (see preceding text for detailed discussion).

Same conclusions can also be made from the drug dissolution profiles (Fig. 8), which was obtained by integrating Eq. 22 (for the predicted profile) and with known true density of succinic acid ( $\rho=1.57\ \text{g}/\text{cm}^3$ , for the experimental profile). As exemplified in Fig. 8, while the experimental dissolution profile is largely in agreement with the prediction obtained from the 3D model, it is significantly faster than the dissolution profile calculated from the 1D, Nernst-Brunner scheme. Taken together, the Nernst-Brunner scheme gives rise to shallower concentration gradient at the surface of the particle, thus significantly under-estimating the particle dissolution rate.

## Practical Significance

Dissolution of drug particles is of utmost importance for the performance of oral solid dosage forms. For over a century, the drug particle dissolution was commonly understood and modeled under the framework of the Noyes-Whitney and Nernst-Brunner equations, the underlying assumption of which being the diffusion-driven process in 1D. We have shown in the preceding text that, in theory, the real-life drug dissolution in the 3D space must differ from the classic 1D model, because the concentration gradient under the 3D consideration cannot be a constant value (aka. linear concentration profile across the diffusion layer). Despite this inherent theoretical deficiency, the classic, 1D-based theory remains to be the conventional wisdom underlying the drug particle dissolution behavior. Its popularity is likely due to the simplicity in understanding, and the fact that the actual drug dissolution rate is infrequently calculated directly from the drug diffusion coefficient and the diffusion layer thickness, by following the Nernst-Brunner equation. In other words, due to the uncertainties involved in estimation of the diffusion layer thickness (25), the Nernst-Brunner formalism is more commonly treated in a semi-empirical fashion, by which the term  $D/h$  is generalized as a dissolution rate constant  $k$ , and the underlying mechanism is only followed in a qualitative or semi-quantitative manner. For this reason, the classic, 1D-based theory serves its purpose despite the lack of full theoretical rigor.

The creation of the dissolution model by considering the drug diffusion in the 3D space, as shown in the preceding sections, makes it possible to reliably estimate the drug dissolution rate with the known drug diffusion coefficient and diffusion layer thickness. It is known that the diffusion layer thickness can be influenced by a number of factors, such as particle size, density, and hydrodynamics of the system. It was shown by multiple empirical models that for suspended particles, the diffusion layer thickness is similar to the particle radius when the particle diameter is less than approximately  $60\ \mu\text{m}$ . Whereas for coarser particles, the diffusion layer thickness remain relatively constant at around  $30\ \mu\text{m}$

(8, 13, 14). At this level of diffusion layer thickness, the discrepancy between the 1D and 3D calculation can be significant. For example, given a typical drug particle with the diameter of 20  $\mu\text{m}$  (diffusion layer thickness is therefore 10  $\mu\text{m}$ ) and the diffusion coefficient identical to the succinic acid ( $D = 8.8 \times 10^{-10} \text{ m}^2/\text{sec}$ ), our study shows that the dissolution time calculated under the 1D condition is longer than under the 3D condition by several folds, regardless of the drug solubility (Fig. 9). As shown in previously, the steady state concentration gradient at the surface of the particle under 3D consideration ( $\left. \frac{\partial C}{\partial r} \right|_{r=a} = \frac{C_s}{h} + \frac{C_s}{a}$ ) differs from the 1D consideration ( $\left. \frac{\partial C}{\partial r} \right|_{r=a} = \frac{C_s}{h}$ ) by an amount equal to  $\frac{C_s}{a}$ . Therefore, for particles suspended in fluid, of which the maximum diffusion layer thickness  $h$  is estimated to be 30  $\mu\text{m}$ , the dissolution times arising from the 1D and 3D-based calculations will begin to converge when the drug particle size is significantly greater than 30  $\mu\text{m}$ , as exemplified in Fig. 10.

Additionally, our model makes it possible to calculate the amount of time it takes to reach the steady-state concentration profile during dissolution. The results show that the rate of achieving the steady-state is diffusion layer thickness-dependent, with longer time required for thicker diffusion layer. For example, for a 400  $\mu\text{m}$  succinic acid particle (radius is 200  $\mu\text{m}$ ) which remains static in a water droplet (i.e.  $h = 200 \mu\text{m}$ ), it takes 21.2 s to reach the steady-state (defined as the length of time required for the concentration gradient at the surface of the particle to reach 101% of the value at the infinite time). In contrast, for the same succinic acid particle suspended in water, the diffusion layer thickness is much lower ( $h \approx 30 \mu\text{m}$ ), and it therefore gives rise to a significantly faster rate to reach the steady-state ( $t = 0.5 \text{ s}$ ). In general, concerning the total dissolution time, the contribution from the non-steady state portion is relatively insignificant, especially for systems where particles are well suspended.

Overall, this study indicates that the Nernst-Brunner formalism could significantly under-predict the dissolution rate in real-life drug dissolution processes. It also suggests that the time needed to reach equilibrium solubility may be shorter

**Fig. 9** Dissolution time as the function of diffusion layer thickness for a succinic acid particle ( $d = 20 \mu\text{m}$ ), with hypothetical solubility of 56 mg/mL (Panel A) and 0.56 mg/mL (Panel B), calculated using the 3D model (red) and the Nernst-Brunner formalism (blue).

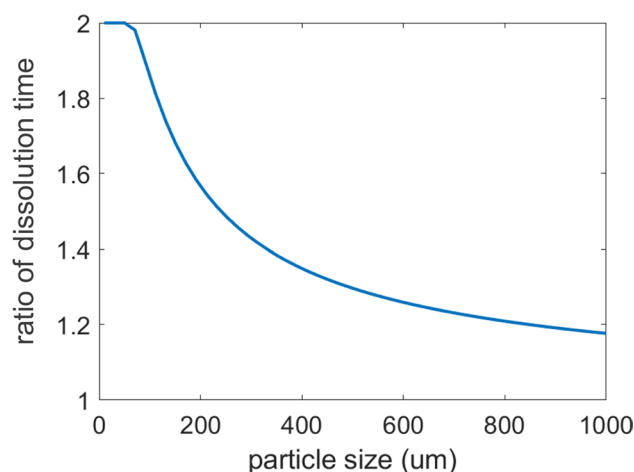
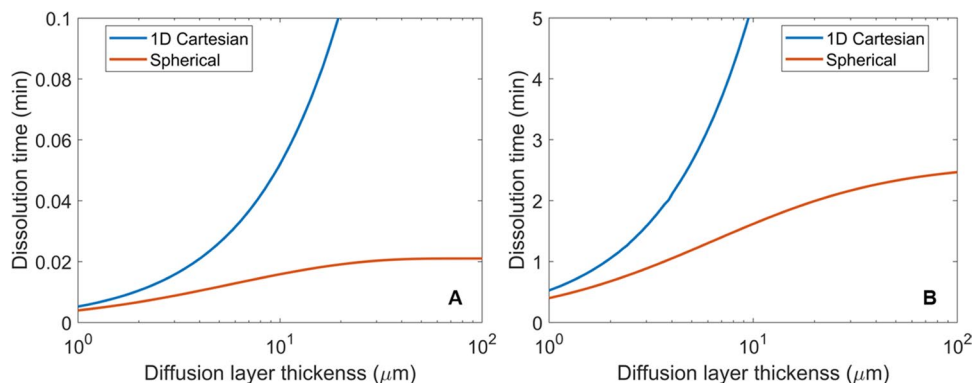


**Fig. 10** Ratio of the calculated dissolution time using the Nernst-Brunner formalism to the calculated dissolution time using the 3D model, as the function of particle size, for succinic acid particles suspended in water.

than anticipated. This study may also help to improve the performance of biopharmaceutics modeling, because the Nernst-Brunner formalism is implicated in most drug dissolution rate calculation in the existing biopharmaceutics models.

The main objective of this study is to introduce the underlying theory and the governing model for drug particle dissolution under the 3D consideration. Hence, the experimental system employed for the model verification was designed specifically for this purpose. Namely, the system exhibits the evolution of single, static particles immersed in un-stirred water during dissolution, such that the diffusion layer thickness is considered to be equal to the particle radius. To further understand the real-life effect of drug dissolution in 3D, the model presented in this study can be extended to encompassing polydispersed particle ensembles and by imposing the dynamic changes of diffusion layer thickness during dissolution (8), such that the behavior of real, bulk dissolution processes can be modeled under the 3D condition. The simulation of the bulk dissolution using the 3D dissolution model will be presented in a follow-up publication.

## Conclusion

Aimed at an enhanced understanding of the drug dissolution process, we developed a drug particle dissolution model with an emphasis of describing the drug dissolution in the 3D space, by considering both the non-steady and steady states. The model was derived by following the same foundational principles as the classic Nernst-Brunner formalism. Namely, particle dissolution is diffusion-driven within the diffusion layer, governed by Fick's laws of diffusion. Rather than treating the model in 1D, the dissolution of a spherical drug particle was modeled by presenting the Fick's second law in 3D, spherical coordinates in this study. By solving the resulting partial differential equation, the drug concentration as the function of time can be determined anywhere within the diffusion layer, and the drug dissolution rate is subsequently obtained. The drug dissolution model was experimentally verified by evaluating the dissolution of single succinic acid particles under a polarized microscope, by which the evolution of the drug particle size was measured by means of image segmentation techniques. The kinetic profiles of the succinic acid particle dissolution are in good agreement with the simulated results, demonstrating the validity of the 3D dissolution model. Notably, simulations considering the 1D condition (Nernst-Brunner formalism) led to substantial under-estimation of the dissolution rate. This discrepancy is caused by the inherent deficiency arising from treating the drug diffusion process in 1D condition, which inevitably leads to a constant concentration profile across the diffusion layer. This outcome deviates from the realistic situation, in which the concentration gradient, in 3D, is not a constant value and is significantly higher at the surface of the particle. Overall, this study implicates that calculation within the framework of the Nernst-Brunner equation may significantly under-predict the drug dissolution rate. The model presented in this study, by treating drug dissolution in 3D space, may provide a more realistic account of the drug dissolution process and potentially a reliable method to simulate the real-life drug dissolution process.

## Declarations

**Conflicts of Interests/Competing Interests** The authors declare that they have no conflicts of interests.

## References

- Dokoumetzidis A, Macheras P. A century of dissolution research: from Noyes and Whitney to the biopharmaceutics classification system. *Int J Pharm.* 2006;321(1–2):1–11.
- Siepmann J, Siepmann F. Mathematical modeling of drug dissolution. *Int J Pharm.* 2013;453(1):12–24.
- Noyes AA, Whitney WR. The rate of solution of solid substances in their own solutions. *J Am Chem Soc.* 1897;19(12):930–4.
- Brunner E. Reaktionsgeschwindigkeit in heterogenen Systemen. *Z Phys Chem.* 1904;47(1):56–102.
- Nernst W. Theorie der Reaktionsgeschwindigkeit in heterogenen Systemen. *Z Phys Chem.* 1904;47(1):52–5.
- Danckwerts P. Significance of liquid-film coefficients in gas absorption. *Ind Eng Chem.* 1951;43(6):1460–7.
- Higuchi T. Rate of release of medicaments from ointment bases containing drugs in suspension. *J Pharm Sci.* 1961;50(10):874–5.
- Hintz RJ, Johnson KC. The effect of particle size distribution on dissolution rate and oral absorption. *Int J Pharm.* 1989;51(1):9–17.
- Lu AT, Frisella ME, Johnson KC. Dissolution modeling: factors affecting the dissolution rates of polydisperse powders. *Pharm Res.* 1993;10(9):1308–14.
- Sugano K. Introduction to computational oral absorption simulation. *Expert Opinion On Drug Metabolism & Toxicology.* 2009;5(3):259–93.
- Ranz W, Marshall WJ. Evaporation from drops Part I. *Chem Eng Prog.* 1952;48:141–6.
- Martin A, Bustamante P, Chun A. Diffusion and Dissolution. In: *Physical Pharmacy.* Philadelphia, PA, USA: Lea & Febiger; 1993. p. 324–361.
- Wang J, Flanagan DR. General solution for diffusion-controlled dissolution of spherical particles. 1. Theory. *Journal of Pharmaceutical Sciences.* 1999;88(7):731–8.
- Wang J, Flanagan DR. General solution for diffusion-controlled dissolution of spherical particles. 2. Evaluation of experimental data. *Journal of Pharmaceutical Sciences.* 2002;91(2):534–42.
- Hixson A, Crowell J. Dependence of reaction velocity upon surface and agitation. *Ind Eng Chem.* 1931;23(8):923–31.
- Hixson A, Crowell J. Dependence of reaction velocity upon surface and agitation. II. Experimental procedure in study of surface. *Ind Eng Chem.* 1931;23:1002–9.
- Crank J. *The Mathematics of Diffusion.* Bristol, UK: Oxford University Press; 1975.
- Korenev BG. *Bessel Functions and Their Applications.* Boca Raton, FL, USA: CRC Press; 2002.
- Boas ML. *Mathematical Methods in the Physical Sciences.* In. Hoboken, NJ, USA: John Wiley & Sons; 2006. p. 340–89.
- Shampine LF, Reichelt MW. The matlab ode suite. *SIAM J Sci Comput.* 1997;18(1):1–22.
- Shorten RB. Approximate Analytic Solution of the One Phase Stefan Problem for the Sphere. In: *IUTAM Symposium on Recent Advances in Moving Boundary Problems in Mechanics.* Cham, Switzerland: Springer International Publishing; 2019. p. 185–201.
- Wu B, McCue SW, Tillman P, Hill JM. Single phase limit for melting nanoparticles. *Appl Math Model.* 2009;33(5):2349–67.
- Hu Y-H, Chen Z-G, Yang W-G, Shi Y, Sun H-L, Li Y-L. Solubility of succinic acid in ethanol plus water systems from 278.15 K to 333.15 K. *Journal of Solution Chemistry.* 2013;42(1):102–10.
- Kim H. Diffusion studies of the systems water-succinic acid-urea and water-succinic acid at 25° C: The effect of complex formation on the diffusion coefficients of the ternary system. *J Solution Chem.* 1974;3(4):271–87.
- Sugano K. *Biopharmaceutics Modeling and Simulations: Theory, Practice, Methods, and Applications.* Hoboken, New Jersey: John Wiley & Sons; 2012.

**Publisher's Note** Springer Nature remains neutral with regard to jurisdictional claims in published maps and institutional affiliations.